Proceedings of the ASME 2013 International Design Engineering Technical Conferences & Computers and Information in Engineering Conference
IDETC/CIE 2013
August 4-7, 2013, Portland, Oregon, USA

DETC2013-12316

ON THE STABILIZABILITY OF THE DELAYED INVERTED PENDULUM CONTROLLED BY FINITE SPECTRUM ASSIGNMENT IN CASE OF PARAMETER UNCERTAINTIES

Tamás G. Molnár
Department of Applied Mechanics, Budapest
University of Technology and Economics
Budapest, Hungary

Tamás Insperger
Department of Applied Mechanics, Budapest
University of Technology and Economics
Budapest, Hungary

ABSTRACT

An application of the Finite Spectrum Assignment (FSA) control technique is presented for an inverted pendulum with feedback delay. The FSA controller predicts the actual state of the system over the delay period using an internal model of the real system. If the internal model is perfectly accurate then the feedback delay can be compensated. However, slight parameter mismatch of the internal model may result in an unstable control process. In this paper, stabilizability of the inverted pendulum for different system and delay parameter mismatches are analyzed. It is shown that, for the same parameter uncertainties, the FSA controller allows stabilization for significantly larger feedback delays than a conventional delayed proportional-derivative controller does. In the analysis, it is assumed that the controller input is piecewise constant (sampled), this way the destabilizing effect of the difference part of the governing neutral functional differential equation is eliminated. The relation of the FSA controller to the Smith predictor is also described in time domain.

1. INTRODUCTION

Control of unstable systems with feedback delay is a challenging problem in engineering and science [19], [12]. Time delay is usually considered to be a source of unstable behavior, which should be eliminated from the control system. An effective way to compensate the destabilizing effect of feedback delays is the application of predictive controllers such as the celebrated Smith Predictor [18] and its modifications [15], the Finite Spectrum Assignment [10], [21], [7], the Reduction Approach [1] or the predictive pole-placement control [3]. The main idea behind predictive controllers is that the feedback delay is eliminated from the control loop using a prediction of the actual state based on an internal model of the plant. A detailed overview on time delay compensation in a more general concept is given in the book [8].

It is a general view that the original Smith Predictor is capable to compensate the feedback delay for stable open-loop systems only. It should be mentioned however that in case of extremely large mismatch between the internal model and the real system, the Smith Predictor can stabilize unstable open-loop plants too [4].

In this paper, we investigate the delay compensation technique called Finite Spectrum Assignment (FSA). While the Smith Predictor is a frequency domain idea, FSA is based on time-domain considerations. The basic idea of the FSA controller is that the state variables are predicted over the delay period using an internal model with the delayed values of the state as initial condition. If the internal model is perfectly accurate then the FSA controller can completely eliminate the delay from the control loop. A drawback of FSA controllers is however that it is very sensitive to implementation inaccuracies and to parameter uncertainties. Actually, the system equations, the control law and the internal model of the FSA controller form a system of Neutral Functional Differential Equations (NFDE), for which the stability analysis requires special care [2], [14], [12].

The goal of this paper is to analyze the stabilizability of the inverted pendulum with feedback delay by the FSA controller in case of internal model mismatches. In addition to being a paradigm in control theory [17], stabilization of the inverted pendulum with feedback delay has a high importance in understanding human balancing and human motor control [15], [13], [20], [9]. It is known that a traditional proportional-derivative (PD) controller cannot stabilize an unstable equilibrium if the feedback delay is larger than a critical value. The critical time delay for an inverted pendulum can be given as

$$\tau = \frac{T_\mathrm{p}}{\pi\sqrt{2}}, \tag{1}$$

where T_p is the period of the small oscillations of the same mechanical structure hanging at its downward position [20]. Theoretically, the FSA controller in case of perfect matching of the internal model can stabilize any unstable systems for any large feedback delay. The limitations are the parameter uncertainties in the internal model, the noise in the sensory input and the problems of the implementation of the control law. In this paper, we analyze the effect of the uncertainties in the internal model on the stabilizability of an inverted pendulum. The structure of the article is as follows. First, the mechanical model is presented in Section 2. Then the time-domain and the frequency-domain representations of the FSA controller is described with special attention to the implementation difficulties in Section 3. Section 4 and 5 presents the analytical and numerical stability analysis of the inverted pendulum subjected to the FSA controller. The effect of parameter uncertainties on the stabilizability are investigated in Section 6. The results are concluded in Section 7.

2. MECHANICAL MODEL

The mechanical model of the inverted pendulum is shown in Figure 1. The pendulum is assumed to be homogenous, the length is *l*, and the mass is *m*. The angular displacement of the pendulum is denoted by φ and the position of the pivot point is *x*. The control force *Q* is acting at the pivot point. The cart is assumed to be frictionless and its mass is assumed to be negligible compared to the mass of the pendulum. The governing equation of motion can be given as

$$\ddot{\varphi}(t) - a\varphi(t) = -q(t-\tau), \tag{2}$$

where $a = 6g/l$ [1/s^2] is the system parameter, $q(t) = 6Q(t)/(ml)$ [1/s^2] is the normalized control force and τ [s] is the feedback delay.

The state space model of the system reads

$$\dot{\mathbf{x}}(t) = \mathbf{A}\mathbf{x}(t) + \mathbf{B}\mathbf{u}(t-\tau), \tag{3}$$

where

$$\mathbf{x}(t) = \begin{pmatrix}\varphi(t)\\ \dot{\varphi}(t)\end{pmatrix},\ \mathbf{A} = \begin{pmatrix}0 & 1\\ a & 0\end{pmatrix},\ \mathbf{B} = \begin{pmatrix}0\\ 1\end{pmatrix},\ \mathbf{u}(t) = -q(t). \tag{4}$$

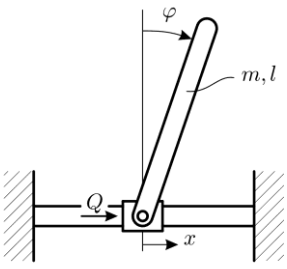

Figure 1. Mechanical model

In case of a PD controller, the control force reads

$$q(t) = k_\mathrm{p}\varphi(t) + k_\mathrm{d}\dot{\varphi}(t), \tag{5}$$

where $k_\mathrm{p} = 6K_\mathrm{p}/(ml)$ [1/s^2] and $k_\mathrm{d} = 6K_\mathrm{d}/(ml)$ [1/s] are the normalized proportional and derivative control gains with K_p and K_d being the actual control gains. It is known that for a given system parameter *a*, the system cannot be stabilized if the feedback delay is larger than the critical value

$$\tau_{\mathrm{crit,PD}} = \sqrt{\frac{2}{a}} = \sqrt{\frac{l}{3g}}. \tag{6}$$

The characteristic equation of the system reads

$$D(\lambda) = \lambda^2 - a + k_\mathrm{p}\mathrm{e}^{-\lambda\tau} + k_\mathrm{d}\lambda\mathrm{e}^{-\lambda\tau}. \tag{7}$$

According to the D-subdivision method, the equation $D(\mathrm{i}\omega) = 0$ gives the D-curves of the system in the form

$$k_\mathrm{p} = a,\ \ k_\mathrm{d} \in \mathbb{R}, \qquad \text{if } \omega = 0, \tag{8}$$

$$k_\mathrm{p} = (\omega^2 + a)\cos(\omega\tau),\quad k_\mathrm{d} = \frac{\omega^2 + a}{\omega}\sin(\omega\tau), \text{ if } \omega \neq 0. \tag{9}$$

Equation (8) corresponds to static loss of stability (a single real characteristic root with zero real part), while Eq. (9) is associated with dynamic loss of stability (a pair of complex characteristic roots with zero real part). The D-curves and stability chart of the system are shown in Figure 2.

3. FINITE SPECTRUM ASSIGNMENT

In order to stabilize the inverted pendulum, the FSA control procedure is used. FSA is a predictive control method, which is supposed to realize pole placement for systems with input delay by using a control law that contains a distributed delay term. FSA allows the realization of a closed-loop system that operates with a predefined dynamic behavior in the ideal case. Time delay compensation can be achieved by the means of prediction and feedback of the predicted state. Thus finitely many poles of the system can be shifted to desired values and the remaining (infinitely many) poles are automatically eliminated.

3.1. Time domain representation

In the course of prediction, the controlled system should be described by a model equation, which is called the internal model of the controller. This equation can be written in the form

$$\dot{\mathbf{x}}(t) = \tilde{\mathbf{A}}\mathbf{x}(t) + \tilde{\mathbf{B}}\mathbf{u}(t-\tilde{\tau}), \tag{10}$$

where $\tilde{\mathbf{A}}$, $\tilde{\mathbf{B}}$ and $\tilde{\tau}$ are the parameters of the state space model of the system in the internal model, i.e.

$$\tilde{\mathbf{A}} = \begin{pmatrix}0 & 1\\ \tilde{a} & 0\end{pmatrix},\quad \tilde{\mathbf{B}} = \begin{pmatrix}0\\ 1\end{pmatrix}. \tag{11}$$

The predictor used in case of FSA approach solves this equation with the initial value $\mathbf{x}(t-\tilde{\tau})$ and formally shifts the

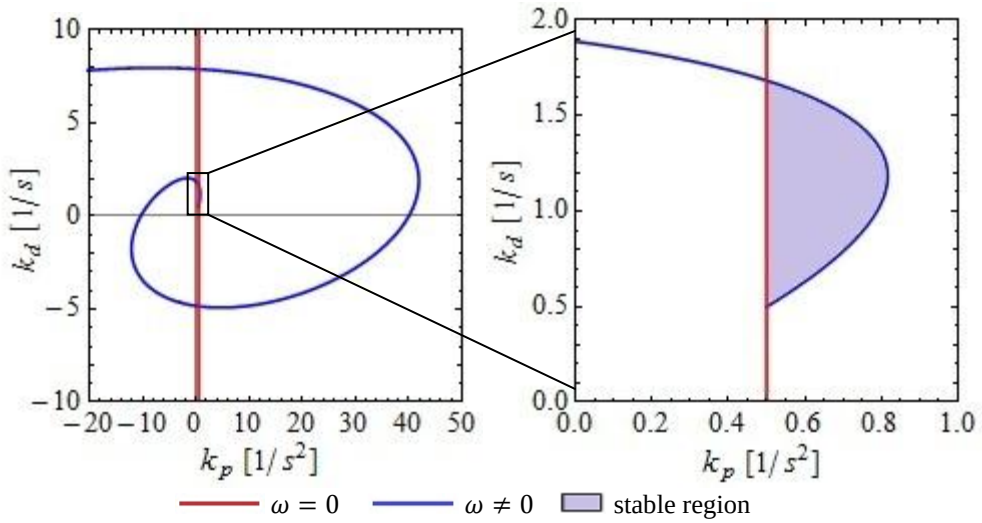

Figure 2. Stability chart of the system (3)-(5) for $\tau = 1$ [s] and $a = 0.5$ [1/s^2].

argument of the solution by $\tilde{\tau}$. This way the predicted state reads

$$\mathbf{x}_\mathrm{p}(t+\tilde{\tau}) = \mathrm{e}^{\tilde{\mathbf{A}}\tilde{\tau}}\mathbf{x}(t) + \int_{-\tilde{\tau}}^{0} \mathrm{e}^{-\tilde{\mathbf{A}}\theta}\,\tilde{\mathbf{B}}\mathbf{u}(t+\theta)\mathrm{d}\theta. \tag{12}$$

The controller uses this predicted state for the feedback. Thus the control signal can be written in the form

$$\mathbf{u}(t) = \mathbf{K}\mathrm{e}^{\tilde{\mathbf{A}}\tilde{\tau}}\mathbf{x}(t) + \mathbf{K}\int_{-\tilde{\tau}}^{0} \mathrm{e}^{-\tilde{\mathbf{A}}\theta}\,\tilde{\mathbf{B}}\mathbf{u}(t+\theta)\mathrm{d}\theta, \tag{13}$$

where $\mathbf{K}$ is the control matrix, which contains the control parameters. In case of a PD controller $\mathbf{K} = (-k_p \quad -k_d)$. The control law (13) is a linear Volterra equation of the second kind and it involves a distributed delay term.

If the internal model is not perfectly accurate (i.e. if $\tilde{\mathbf{A}} \neq \mathbf{A}$, $\tilde{\mathbf{B}} \neq \mathbf{B}$ and $\tilde{\tau} \neq \tau$), then Eqs. (3) and (13) form a system of NFDEs since Eq. (13) is a difference equation for the input $\mathbf{u}$ [2], [14].

If $\tilde{\mathbf{B}} = \mathbf{B}$ (which is the case for the inverted pendulum), then Eqs. (3) and (13) imply

$$\dot{\mathbf{x}}(t) = \mathbf{A}\mathbf{x}(t) + \mathbf{B}\left[\mathbf{K}\mathrm{e}^{\tilde{\mathbf{A}}\tilde{\tau}}\mathbf{x}(t-\tau) + \mathbf{K}\int_{-\tilde{\tau}}^{0} \mathrm{e}^{-\tilde{\mathbf{A}}\theta}\,\mathbf{B}\mathbf{u}(t-\tau+\theta)\mathrm{d}\theta\right]. \tag{14}$$

Using Eq. (3) for the term $\mathbf{B}\mathbf{u}(t-\tau+\theta)$ and substitution into the integral in (14) yields the differential equation for the closed control loop system in the form

$$\dot{\mathbf{x}}(t) = \mathbf{A}\mathbf{x}(t) + \mathbf{B}\mathbf{K}\mathrm{e}^{\tilde{\mathbf{A}}\tilde{\tau}}\mathbf{x}(t-\tau) + \mathbf{B}\mathbf{K}\int_{-\tilde{\tau}}^{0} \mathrm{e}^{-\tilde{\mathbf{A}}\theta}\left(\dot{\mathbf{x}}(t+\theta) - \mathbf{A}\mathbf{x}(t+\theta)\right)\mathrm{d}\theta. \tag{15}$$

It can be observed, that (15) is a NFDE, because the rate of change of state depends on its own past values. Therefore the spectrum of the system described by (15) is infinite.

In the ideal case the internal model approximates the system parameters with perfect precision, i.e. $\tilde{\mathbf{A}} = \mathbf{A}$, $\tilde{\tau} = \tau$. In this case the integral term in (15) can be simplified and the following ordinary differential equation can be obtained

$$\dot{\mathbf{x}}(t) = \mathbf{A}\mathbf{x}(t) + \mathbf{B}\mathbf{K}\mathbf{x}(t). \tag{16}$$

Thus the feedback delay is eliminated from the control loop, hence the spectrum of the closed-loop system becomes finite and the poles can be shifted to any desired values. This way stability can be achieved for arbitrary system parameters.

However, if the parameters in the internal model do not match the real system parameters ($\tilde{\mathbf{A}} \neq \mathbf{A}$, $\tilde{\tau} \neq \tau$), then stability is described by Eqs. (3) and (13).

3.2. Frequency domain representation

The control procedure can be described in frequency domain using Laplace transformation. The Laplace transform of Eq. (3) reads

$$s\mathbf{X}(s) - \mathbf{X}_0 = \mathbf{A}\mathbf{X}(s) + \mathbf{B}\mathrm{e}^{-s\tau}\mathbf{U}(s), \tag{17}$$

$$\mathbf{X}(s) = (s\mathbf{I} - \mathbf{A})^{-1}\mathbf{B}\mathrm{e}^{-s\tau}\mathbf{U}(s) + (s\mathbf{I} - \mathbf{A})^{-1}\mathbf{X}_0, \tag{18}$$

where s is the Laplace operator, $\mathbf{I}$ is the identity matrix, and $\mathbf{X}_0$ is the initial value of $\mathbf{x}(t)$ at $t = t_0$.

The Laplace transform of Eq. (13) reads

$$\mathbf{U}(s) = \mathbf{K}\mathrm{e}^{\tilde{\mathbf{A}}\tilde{\tau}}\mathbf{X}(s) + \mathbf{K}\int_{-\tilde{\tau}}^{0} \mathrm{e}^{-\tilde{\mathbf{A}}\theta}\,\tilde{\mathbf{B}}\mathrm{e}^{s\theta}\mathbf{U}(s)\mathrm{d}\theta, \tag{19}$$

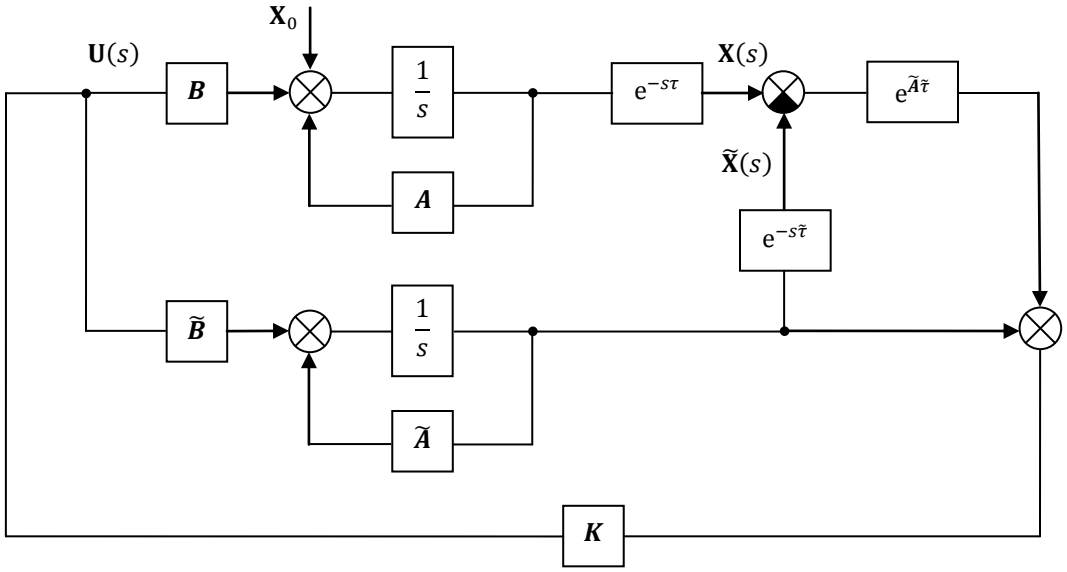

Figure 3. The block diagram of the FSA controller.

$$\mathbf{U}(s) = \mathbf{K}\mathrm{e}^{\tilde{\mathbf{A}}\tilde{\tau}}\mathbf{X}(s) + \mathbf{K}\left(s\mathbf{I} - \tilde{\mathbf{A}}\right)^{-1}\tilde{\mathbf{B}}\mathbf{U}(s) - \mathbf{K}\left(s\mathbf{I} - \tilde{\mathbf{A}}\right)^{-1}\mathrm{e}^{-(s\mathbf{I}-\tilde{\mathbf{A}})\tilde{\tau}}\tilde{\mathbf{B}}\mathbf{U}(s)\,. \tag{20}$$

Using the identity $\left(s\mathbf{I} - \tilde{\mathbf{A}}\right)^{-1}\mathrm{e}^{\tilde{\mathbf{A}}\tilde{\tau}} = \mathrm{e}^{\tilde{\mathbf{A}}\tilde{\tau}}\left(s\mathbf{I} - \tilde{\mathbf{A}}\right)^{-1}$, Eq. (20) can be written in the form

$$\mathbf{U}(s) = \mathbf{K}\Big(\left(s\mathbf{I} - \tilde{\mathbf{A}}\right)^{-1}\tilde{\mathbf{B}}\mathbf{U}(s) + \mathrm{e}^{\tilde{\mathbf{A}}\tilde{\tau}}\left(\mathbf{X}(s) - \left(s\mathbf{I} - \tilde{\mathbf{A}}\right)^{-1}\tilde{\mathbf{B}}\mathrm{e}^{-s\tilde{\tau}}\mathbf{U}(s)\right)\Big). \tag{21}$$

The block diagram of the closed control loop realizing $\mathbf{x}(t) \equiv \mathbf{0}$ can be constructed using Eqs. (18) and (21). The block diagram is shown in Figure 3. It can be observed that the state variables $\mathbf{X}(s)$ of the real system and the state variables $\tilde{\mathbf{X}}(s)$ of the model system used for prediction are calculated in a similar way. The line without the term $\mathrm{e}^{-s\tilde{\tau}}$ shows the realization of the prediction and $\mathbf{K}$ denotes the feedback control gain.

The block diagram of the FSA control method is similar to that of the Smith Predictor. The only difference is that the block $\mathrm{e}^{\tilde{\mathbf{A}}\tilde{\tau}}$ in the line of $\mathbf{X}(s) - \tilde{\mathbf{X}}(s)$ is not present in the Smith Predictor's block diagram. The reason for this is that in pursuance of prediction the Smith Predictor always uses $\mathbf{x}(0)$ as initial state while the FSA uses a prediction over the delay interval only with the initial state $\mathbf{x}(t - \tilde{\tau})$.

3.3. Problems with the realization of the controller

In order to implement the control procedure in practice, one must perform the online calculation of the integral term in control law (13). Let this integral term be denoted by

$$\mathbf{z}(t) = \int_{-\tilde{\tau}}^{0} \mathrm{e}^{-\tilde{\mathbf{A}}\theta}\,\tilde{\mathbf{B}}\mathbf{u}(t+\theta)\mathrm{d}\theta. \tag{22}$$

One solution for realizing $\mathbf{z}(t)$ is to create a differential equation by deriving Eq. (22). The differential equation reads

$$\dot{\mathbf{z}}(t) = \tilde{\mathbf{B}}\mathbf{u}(t) - \mathrm{e}^{\tilde{\mathbf{A}}\tilde{\tau}}\tilde{\mathbf{B}}\mathbf{u}(t-\tilde{\tau}) + \tilde{\mathbf{A}}\mathbf{z}(t). \tag{23}$$

It is known that this type of realization involves unstable pole-zero cancellation if matrix $\mathbf{A}$ is not Hurwitz, hence it is not capable of stabilizing an unstable system like the inverted pendulum [10], [14], [12]. Thereby the realization by the help of the described block diagram will not lead to a stable closed-loop system.

Another way to realize the integral term $\mathbf{z}(t)$ is the approximation by a numerical quadrature. In this case the distributed delay term is substituted by a sum of point delays. This way no unstable pole-zero cancellation takes place. A discretized rectangular approximation of $\mathbf{z}(t)$ can be given as

$$\mathbf{z}(t) \cong \sum_{j=0}^{\tilde{r}} \mathrm{e}^{\tilde{\mathbf{A}}j\Delta t}\tilde{\mathbf{B}}\mathbf{u}(t - j\Delta t)\Delta t. \tag{24}$$

where $\Delta t = \tilde{\tau}/\tilde{r}$ is the discrete time step and $\tilde{r}$ is an integer approximation parameter (i.e. the resolution of the interval $[0, \tilde{\tau}]$). The corresponding control law reads

$$\mathbf{u}(t) = \mathbf{K}\mathrm{e}^{\tilde{\mathbf{A}}\tilde{\tau}}\mathbf{x}(t) + \mathbf{K}\sum_{j=0}^{\tilde{r}} \mathrm{e}^{\tilde{\mathbf{A}}j\Delta t}\tilde{\mathbf{B}}\mathbf{u}(t - j\Delta t)\Delta t. \tag{25}$$

Although such a realization of the control law is convenient numerically, it presents a limitation in the stability of the

closed-loop system. Note that Eqs. (3) and (25) form a system of Neutral Differential Difference Equation.

As it was shown in [14], a necessary condition for the stability of the closed-loop system described by Eqs. (3) and (25) is the stability of the difference part of the original NFDE given by (3) and (13), which can be written as

$$\begin{aligned}\mathbf{u}(t) &= \mathbf{K}\mathrm{e}^{\widetilde{\mathbf{A}}\tilde{\tau}}\mathbf{x}(t) + \mathbf{K}\int_{-\tilde{\tau}}^{0}\mathrm{e}^{-\widetilde{\mathbf{A}}\theta}\widetilde{\mathbf{B}}\mathbf{u}(t+\theta)\,\mathrm{d}\theta,\\ \mathbf{x}(t) &\equiv \mathbf{0}.\end{aligned} \tag{26}$$

Alternatively, if $\widetilde{\mathbf{B}} = \mathbf{B}$ then Eq. (15) gives the difference part in the form

$$\dot{\mathbf{x}}(t) = \mathbf{B}\mathbf{K}\int_{-\tilde{\tau}}^{0}\mathrm{e}^{-\widetilde{\mathbf{A}}\theta}\dot{\mathbf{x}}(t+\theta)\,\mathrm{d}\theta. \tag{27}$$

A stable control process can only be obtained if the closed control loop is stable (this condition requires a sufficiently accurate internal model and an accurate implementation of the control law), and if the difference part is stable. For the case of a single-input system the necessary and sufficient condition for stability was given in [11] in the form

$$S = \int_{0}^{\tilde{\tau}}\left|\mathbf{K}^{\mathrm{T}}\mathrm{e}^{\widetilde{\mathbf{A}}\theta}\widetilde{\mathbf{B}}\right|\mathrm{d}\theta < 1. \tag{28}$$

As it was pointed out in [12], the restriction by the difference part can be removed by adding a low-pass filter or by using piecewise constant input, for instance by applying a digital controller.

4. STABILITY ANALYSIS BY THE D-SUBDIVISION METHOD

The stability of the control system can be analyzed using the D-subdivision method and Stepan's formulas [19] for the characteristic equation as it is shown below.

4.1. Stability of the ideal control system

Based on Eqs. (4) and (13) the input signal to control the inverted pendulum by the FSA technique can be given as

$$\begin{aligned}u(t) = {} & (-k_p \quad -k_d)\begin{pmatrix}\mathrm{ch}(\tilde{\alpha}\tilde{\tau}) & \frac{1}{\tilde{\alpha}}\mathrm{sh}(\tilde{\alpha}\tilde{\tau})\\ \tilde{\alpha}\mathrm{sh}(\tilde{\alpha}\tilde{\tau}) & \mathrm{ch}(\tilde{\alpha}\tilde{\tau})\end{pmatrix}\begin{pmatrix}\varphi(t)\\ \dot{\varphi}(t)\end{pmatrix}\\ & +(-k_p \quad -k_d)\int_{-\tilde{\tau}}^{0}\begin{pmatrix}\mathrm{ch}(\tilde{\alpha}\theta) & -\frac{1}{\tilde{\alpha}}\mathrm{sh}(\tilde{\alpha}\theta)\\ -\tilde{\alpha}\mathrm{sh}(\tilde{\alpha}\theta) & \mathrm{ch}(\tilde{\alpha}\theta)\end{pmatrix}\begin{pmatrix}0\\ 1\end{pmatrix}u(t+\theta)\mathrm{d}\theta,\end{aligned} \tag{29}$$

where $\tilde{\alpha} = \sqrt{\tilde{a}}$, ch and sh indicates cosh and sinh. Here, k_p and k_d are the proportional and derivative control gains for the predicted state.

The solutions for system (3) and (29) are assumed to be in the form

$$\varphi(t) = \varphi_0\mathrm{e}^{\lambda t}, \quad \dot{\varphi}(t) = \omega_0\mathrm{e}^{\lambda t}, \quad u(t) = u_0\mathrm{e}^{\lambda t}. \tag{30}$$

Substitution of expressions (30) into Eqs. (3) and (29) gives the following equations

$$\mathbf{M}(\lambda)\begin{pmatrix}\varphi_0\\ \omega_0\\ u_0\end{pmatrix} = \mathbf{0}, \tag{31}$$

$$\mathbf{M}(\lambda) = \begin{pmatrix}\lambda & -1 & 0\\ -\alpha^2 & \lambda & -\mathrm{e}^{-\lambda\tau}\\ k_p\mathrm{ch}(\tilde{\alpha}\tilde{\tau}) + k_d\tilde{\alpha}\mathrm{sh}(\tilde{\alpha}\tilde{\tau}) & \frac{k_p}{\tilde{\alpha}}\mathrm{sh}(\tilde{\alpha}\tilde{\tau}) + k_d\mathrm{ch}(\tilde{\alpha}\tilde{\tau}) & f(\lambda)\end{pmatrix}, \tag{32}$$

$$\begin{aligned}f(\lambda) = {} & 1 + \frac{k_p}{2\tilde{\alpha}}\left(\frac{\mathrm{e}^{-(\lambda+\tilde{\alpha})\tilde{\tau}} - 1}{\lambda+\tilde{\alpha}} + \frac{-\mathrm{e}^{-(\lambda-\tilde{\alpha})\tilde{\tau}} + 1}{\lambda-\tilde{\alpha}}\right)\\ & + \frac{k_d}{2}\left(\frac{-\mathrm{e}^{-(\lambda+\tilde{\alpha})\tilde{\tau}} + 1}{\lambda+\tilde{\alpha}} + \frac{-\mathrm{e}^{-(\lambda-\tilde{\alpha})\tilde{\tau}} + 1}{\lambda-\tilde{\alpha}}\right),\end{aligned} \tag{33}$$

where $\alpha = \sqrt{a}$. Hence the characteristic equation of system (3) and (29) reads

$$D(\lambda) = \det(\mathbf{M}(\lambda)) = 0. \tag{34}$$

Substitution of $\lambda = \mathrm{i}\omega$ into Eq. (34) and decomposition into real and imaginary parts give a linear system of equation for k_p and k_d in the form

$$\begin{aligned}R(\omega) = {} & -(\alpha^2+\omega^2) + k_p\frac{\omega}{\tilde{\alpha}}\sin(\omega\tau)\mathrm{sh}(\tilde{\alpha}\tilde{\tau}) + k_p\cos(\omega\tau)\mathrm{ch}(\tilde{\alpha}\tilde{\tau})\\ & + k_p\frac{\alpha^2+\omega^2}{\tilde{\alpha}^2+\omega^2}\left(1 - \cos(\omega\tilde{\tau})\mathrm{ch}(\tilde{\alpha}\tilde{\tau}) - \frac{\omega}{\tilde{\alpha}}\sin(\omega\tilde{\tau})\mathrm{sh}(\tilde{\alpha}\tilde{\tau})\right)\\ & + k_d\frac{\alpha^2+\omega^2}{\tilde{\alpha}^2+\omega^2}\left(-\tilde{\alpha}\cos(\omega\tilde{\tau})\mathrm{sh}(\tilde{\alpha}\tilde{\tau}) - \omega\sin(\omega\tilde{\tau})\mathrm{ch}(\tilde{\alpha}\tilde{\tau})\right)\\ & + k_d\omega\sin(\omega\tau)\mathrm{ch}(\tilde{\alpha}\tilde{\tau}) + k_d\tilde{\alpha}\cos(\omega\tau)\mathrm{sh}(\tilde{\alpha}\tilde{\tau}) = 0,\end{aligned} \tag{35}$$

$$\begin{aligned}S(\omega) = {} & k_p\frac{\omega}{\tilde{\alpha}}\cos(\omega\tau)\mathrm{sh}(\tilde{\alpha}\tilde{\tau}) - k_p\sin(\omega\tau)\mathrm{ch}(\tilde{\alpha}\tilde{\tau})\\ & + k_p\frac{\alpha^2+\omega^2}{\tilde{\alpha}^2+\omega^2}\left(\sin(\omega\tilde{\tau})\mathrm{ch}(\tilde{\alpha}\tilde{\tau}) - \frac{\omega}{\tilde{\alpha}}\cos(\omega\tilde{\tau})\mathrm{sh}(\tilde{\alpha}\tilde{\tau})\right)\\ & + k_d\frac{\alpha^2+\omega^2}{\tilde{\alpha}^2+\omega^2}\left(\omega + \tilde{\alpha}\sin(\omega\tilde{\tau})\mathrm{sh}(\tilde{\alpha}\tilde{\tau}) - \omega\cos(\omega\tilde{\tau})\mathrm{ch}(\tilde{\alpha}\tilde{\tau})\right)\\ & + k_d\omega\cos(\omega\tau)\mathrm{ch}(\tilde{\alpha}\tilde{\tau}) - k_d\tilde{\alpha}\sin(\omega\tau)\mathrm{sh}(\tilde{\alpha}\tilde{\tau}) = 0.\end{aligned} \tag{36}$$

Expressing k_p and k_d from Eqs. (35) and (36) gives the D-curves for the cases $\omega = 0$ and $\omega \neq 0$, which can be depicted in the plane (k_p, k_d). The regions divided by the D-curves are associated with the same number of unstable characteristic exponents (also called instability degree). This number can be calculated by Stepan's formulas [19]. If the order of the system is even, i.e. $\mathbf{x}(t) \in \mathbb{R}^n$ with $n = 2m$, then the instability degree is

$$N = m + (-1)^m\sum_{k=1}^{r}(-1)^{k+1}\mathrm{sgn}\,S(\rho_k), \tag{37}$$

where $\rho_1 \geq \cdots \geq \rho_r$ are the positive real roots of $R(\omega)$. In case of an odd-order system, i.e. if $\mathbf{x}(t) \in \mathbb{R}^n$ with $n = 2m+1$, then the number of unstable poles is

$$N = m + \frac{1}{2} + (-1)^m \left(\frac{1}{2}(-1)^s \operatorname{sgn} R(0) + \sum_{k=1}^{s-1} (-1)^k \operatorname{sgn} R(\sigma_k) \right), \tag{38}$$

where $\sigma_1 \geq \cdots \geq \sigma_s$ are the nonnegative real roots of $S(\omega)$.

4.2. Stability of the difference part

Substitution of $u(t) = u_0 e^{\lambda t}$ and $\mathbf{x}(t) \equiv \mathbf{0}$ into Eq. (29) gives the characteristic equation of the difference part

$$f(\lambda) = 0. \tag{39}$$

Substitution of $\lambda = \mathrm{i}\omega$ into Eq. (39) and decomposition into real and imaginary parts give

$$\frac{\tilde{\alpha}}{\tilde{\alpha}^2 + \omega^2} \left(\frac{k_p}{\tilde{\alpha}} \cos(\omega\tilde{\tau}) \mathrm{ch}(\tilde{\alpha}\tilde{\tau}) + k_d \cos(\omega\tilde{\tau}) \mathrm{sh}(\tilde{\alpha}\tilde{\tau}) - \frac{k_p}{\tilde{\alpha}} + \frac{k_p \omega}{\tilde{\alpha}^2} \sin(\omega\tilde{\tau}) \mathrm{sh}(\tilde{\alpha}\tilde{\tau}) + \frac{k_d \omega}{\tilde{\alpha}} \sin(\omega\tilde{\tau}) \mathrm{ch}(\tilde{\alpha}\tilde{\tau}) \right) + 1 = 0, \tag{40}$$

$$\frac{\omega}{\tilde{\alpha}^2 + \omega^2} \left(-k_d + \frac{k_p}{\tilde{\alpha}} \cos(\omega\tilde{\tau}) \mathrm{sh}(\tilde{\alpha}\tilde{\tau}) + k_d \cos(\omega\tilde{\tau}) \mathrm{ch}(\tilde{\alpha}\tilde{\tau}) - \frac{k_p}{\omega} \sin(\omega\tilde{\tau}) \mathrm{ch}(\tilde{\alpha}\tilde{\tau}) - \frac{k_d \tilde{\alpha}}{\omega} \sin(\omega\tilde{\tau}) \mathrm{sh}(\tilde{\alpha}\tilde{\tau}) \right) = 0. \tag{41}$$

The D-curves of the difference part can be given by solving these equations for k_p and k_d.

If $\omega = 0$ then Eqs. (40)-(41) give

$$k_d = \frac{1 - \mathrm{ch}(\tilde{\alpha}\tilde{\tau})}{\tilde{\alpha} \mathrm{sh}(\tilde{\alpha}\tilde{\tau})} k_p - \frac{\tilde{\alpha}}{\mathrm{sh}(\tilde{\alpha}\tilde{\tau})}. \tag{42}$$

If $\omega \neq 0$ then one gets

$$k_p = \frac{\tilde{\alpha}(\tilde{\alpha}^2 + \omega^2)\left(\omega - \omega\cos(\omega\tilde{\tau})\mathrm{ch}(\tilde{\alpha}\tilde{\tau}) + \tilde{\alpha}\sin(\omega\tilde{\tau})\mathrm{sh}(\tilde{\alpha}\tilde{\tau})\right)}{2\tilde{\alpha}\omega - 2\tilde{\alpha}\omega\cos(\omega\tilde{\tau})\mathrm{ch}(\tilde{\alpha}\tilde{\tau}) + (\tilde{\alpha}^2 - \omega^2)\sin(\omega\tilde{\tau})\mathrm{sh}(\tilde{\alpha}\tilde{\tau})}, \tag{43}$$

$$k_d = \frac{(\tilde{\alpha}^2 + \omega^2)\left(\tilde{\alpha}\sin(\omega\tilde{\tau})\mathrm{ch}(\tilde{\alpha}\tilde{\tau}) - \omega\cos(\omega\tilde{\tau})\mathrm{sh}(\tilde{\alpha}\tilde{\tau})\right)}{2\tilde{\alpha}\omega - 2\tilde{\alpha}\omega\cos(\omega\tilde{\tau})\mathrm{ch}(\tilde{\alpha}\tilde{\tau}) + (\tilde{\alpha}^2 - \omega^2)\sin(\omega\tilde{\tau})\mathrm{sh}(\tilde{\alpha}\tilde{\tau})}. \tag{44}$$

If the approximation described by (24) is used to realize the control law, then the region of stability in the plane (k_p, k_d) is given by the intersection of the stable regions of the ideal control system (3) and (29) and that of the difference part (26). However if a digital controller is used, then the difference part has no effect on stability.

4.3. Stability diagrams

The stability diagram of the overall control system is given by the superposition of the stability diagram for the ideal control system and the stability diagram for the controller (the difference part) [14]. Figure 4 shows from left to right the stability diagrams for the ideal control system, the stability diagram for the controller, and their superposition for the case when the internal model is perfectly accurate, i.e. when $\tilde{\alpha} = a$ and $\tilde{\tau} = \tau$. The stable domains are indicated by gray shading and the instability degrees of each region are presented. The stability condition for the ideal control system (left panel in Figure 4) is $k_p > a$ and $k_d > 0$, which corresponds to the stability condition for the delay free system. The stability region for the overall control system is however reduced to the small triangular shape region indicated by gray shading in the right panel in Figure 4. In the domain indicated by red color the ideal control system is stable, but the difference part is unstable, thus the overall control loop becomes unstable for any slight imperfections in the implementation of the control law. It is shown in this figure, that a finite spectrum is achieved only for the ideal control system (left panel).

If the internal model is not perfectly accurate, i.e. if $\tilde{\alpha} \neq a$ and $\tilde{\tau} \neq \tau$, then the spectrum becomes infinite and the stable region shrinks as it is shown in Figure 5.

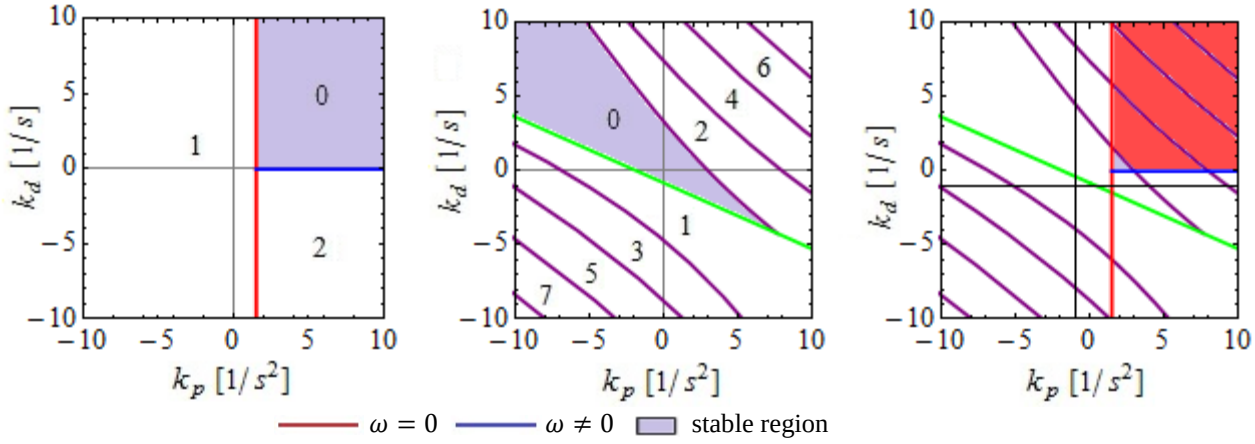

Figure 4. Stability charts of the ideal control system (left), the controller (i.e. the difference part) (middle) and their superposition (right) for system (3)-(29) with $\tilde{\alpha} = a = 1.5$ [1/s^2] and $\tilde{\tau} = \tau = 1$ [s].

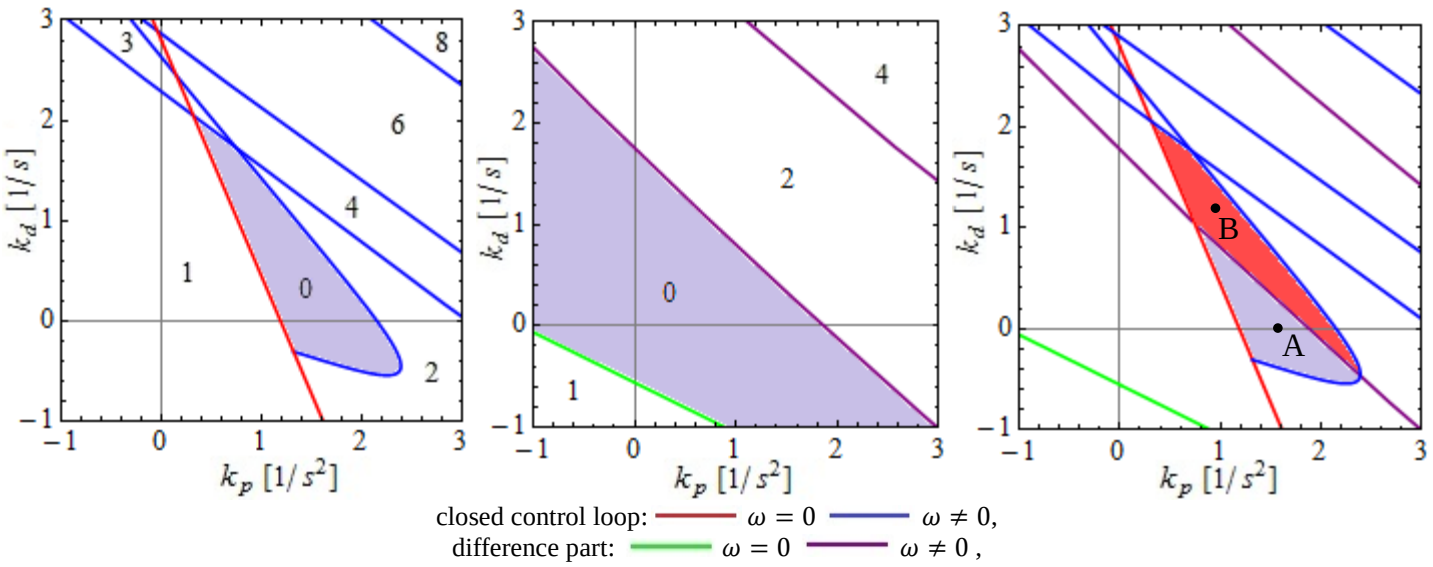

Figure 5. Stability charts of the ideal control system (left), the controller (i.e. the difference part) (middle) and their superposition (right) for system (3)-(29) with $a = 1.5$ [1/s^2], $\tilde{a} = 1.2a$, $\tau = 1$ [s] and $\tilde{\tau} = 1.2\tau$.

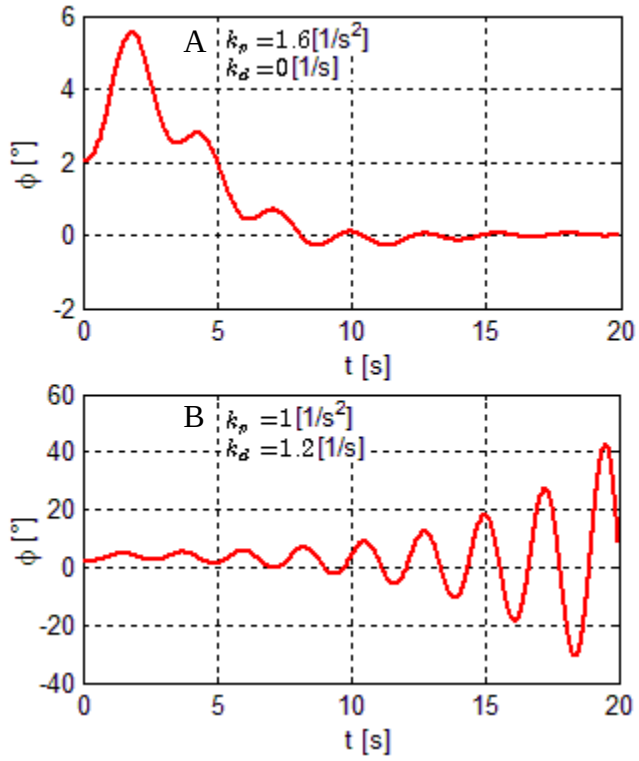

Figure 6. Time domain simulation for the system (3) and (29) with $a = 1.5$ [1/s^2], $\tilde{a} = 1.2a$, $\tau = 1$ [s], $\tilde{\tau} = 1.2\tau$, $\varphi_0 = 2$ [°], and $\omega_0 = 0$.

Figure 6 shows the time domain simulations for parameter points A (stable ideal control system with stable difference part) and B (stable ideal control system with unstable difference part) in Figure 5.

5. APPLICATION OF DIGITAL CONTROLLER

If a digital controller is applied with sampling period Δt [s], then the governing equations read

$$\dot{\mathbf{x}}(t) = \mathbf{A}\mathbf{x}(t) + \mathbf{B}\mathbf{u}(t_{i-r}), \quad t \in [t_i, t_{i+1}), \tag{45}$$

$$\mathbf{u}(t) = \tilde{\mathbf{F}}\mathbf{x}(t_i) + \sum_{j=1}^{\tilde{r}} \tilde{\mathbf{Q}}_j \mathbf{u}(t_{i-j}), \quad t \in [t_i, t_{i+1}), \tag{46}$$

where $t_i = i\Delta t$ $(i = 1,2,3, ...)$, $r = \text{ceil}(\tau/\Delta t)$, $\tilde{r} = \text{ceil}(\tilde{\tau}/\Delta t)$, $\tilde{\mathbf{F}} = \mathbf{K}e^{\tilde{\mathbf{A}}\tilde{\tau}}$, and $\tilde{\mathbf{Q}}_j = \tilde{\mathbf{F}}e^{-\tilde{\mathbf{A}}\tilde{\tau}}e^{\tilde{\mathbf{A}}j\Delta t}\tilde{\mathbf{B}}\Delta t$.

Using state augmentation method and the notations $\mathbf{u}_i = \mathbf{u}(t_i)$ and $\mathbf{x}_i = \mathbf{x}(t_i)$, Eqs. (45) and (46) can be written in one of the following forms. If $r > \tilde{r}$ then

$$\begin{pmatrix} \mathbf{x}_{i+1} \\ \mathbf{u}_i \\ \mathbf{u}_{i-1} \\ \vdots \\ \mathbf{u}_{i-r+1} \end{pmatrix} = \begin{pmatrix} \mathbf{P} & \mathbf{0} & \cdots & \mathbf{0} & \mathbf{0} & \cdots & \mathbf{0} & \mathbf{R} \\ \tilde{\mathbf{F}} & \tilde{\mathbf{Q}}_1 & \cdots & \tilde{\mathbf{Q}}_{\tilde{r}} & \mathbf{0} & \cdots & \mathbf{0} & \mathbf{0} \\ \mathbf{0} & \mathbf{I} & & \cdots & & & \mathbf{0} & \mathbf{0} \\ \vdots & \vdots & & \ddots & & & \vdots & \vdots \\ \mathbf{0} & \mathbf{0} & & \cdots & & & \mathbf{I} & \mathbf{0} \end{pmatrix} \begin{pmatrix} \mathbf{x}_i \\ \mathbf{u}_{i-1} \\ \vdots \\ \mathbf{u}_{i-\tilde{r}} \\ \mathbf{u}_{i-\tilde{r}-1} \\ \vdots \\ \mathbf{u}_{i-r+1} \\ \mathbf{u}_{i-r} \end{pmatrix}, \tag{47}$$

where $\mathbf{P} = e^{\mathbf{A}\Delta t}$ and $\mathbf{R} = \int_0^{\Delta t} e^{\mathbf{A}(\Delta t - \theta)}\mathbf{B}d\theta$. If $r < \tilde{r}$ then

$$\begin{pmatrix} \mathbf{x}_{i+1} \\ \mathbf{u}_i \\ \mathbf{u}_{i-1} \\ \vdots \\ \mathbf{u}_{i-\tilde{r}+1} \end{pmatrix} = \begin{pmatrix} \mathbf{P} & \mathbf{0} & \cdots & \mathbf{0} & \mathbf{R} & \cdots & \mathbf{0} & \mathbf{0} \\ \tilde{\mathbf{F}} & \tilde{\mathbf{Q}}_1 & \cdots & \tilde{\mathbf{Q}}_{r-1} & \tilde{\mathbf{Q}}_r & \cdots & \tilde{\mathbf{Q}}_{\tilde{r}-1} & \tilde{\mathbf{Q}}_{\tilde{r}} \\ \mathbf{0} & \mathbf{I} & & \cdots & & & \mathbf{0} & \mathbf{0} \\ \vdots & \vdots & & \ddots & & & \vdots & \vdots \\ \mathbf{0} & \mathbf{0} & & \cdots & & & \mathbf{I} & \mathbf{0} \end{pmatrix} \begin{pmatrix} \mathbf{x}_i \\ \mathbf{u}_{i-1} \\ \vdots \\ \mathbf{u}_{i-r+1} \\ \mathbf{u}_{i-r} \\ \vdots \\ \mathbf{u}_{i-\tilde{r}+1} \\ \mathbf{u}_{i-\tilde{r}} \end{pmatrix}. \quad (48)$$

These equations are of the form $\mathbf{y}_{i+1} = \mathbf{\Phi}\mathbf{y}_i$, thus the stability of the system can be determined by the analysis of the eigenvalues of the coefficient matrix $\mathbf{\Phi}$, which is in fact the monodromy matrix. The condition for asymptotic stability reads

$$\max(|\mathrm{eig}(\mathbf{\Phi})|) < 1. \quad (49)$$

In the case of a digital controller, the difference part has no effect on stability, thus the stability can be determined by the Eq. (49) only.

In fact, discrete maps (47) and (48) correspond to the semi-discretization of the original continuous system described by Eqs. (3) and (13) with the discretization step being the sampling period Δt [6]. For sufficiently small Δt, the stability properties of the discrete maps (47) and (48) are the same as that of the original continuous system (3) and (13).

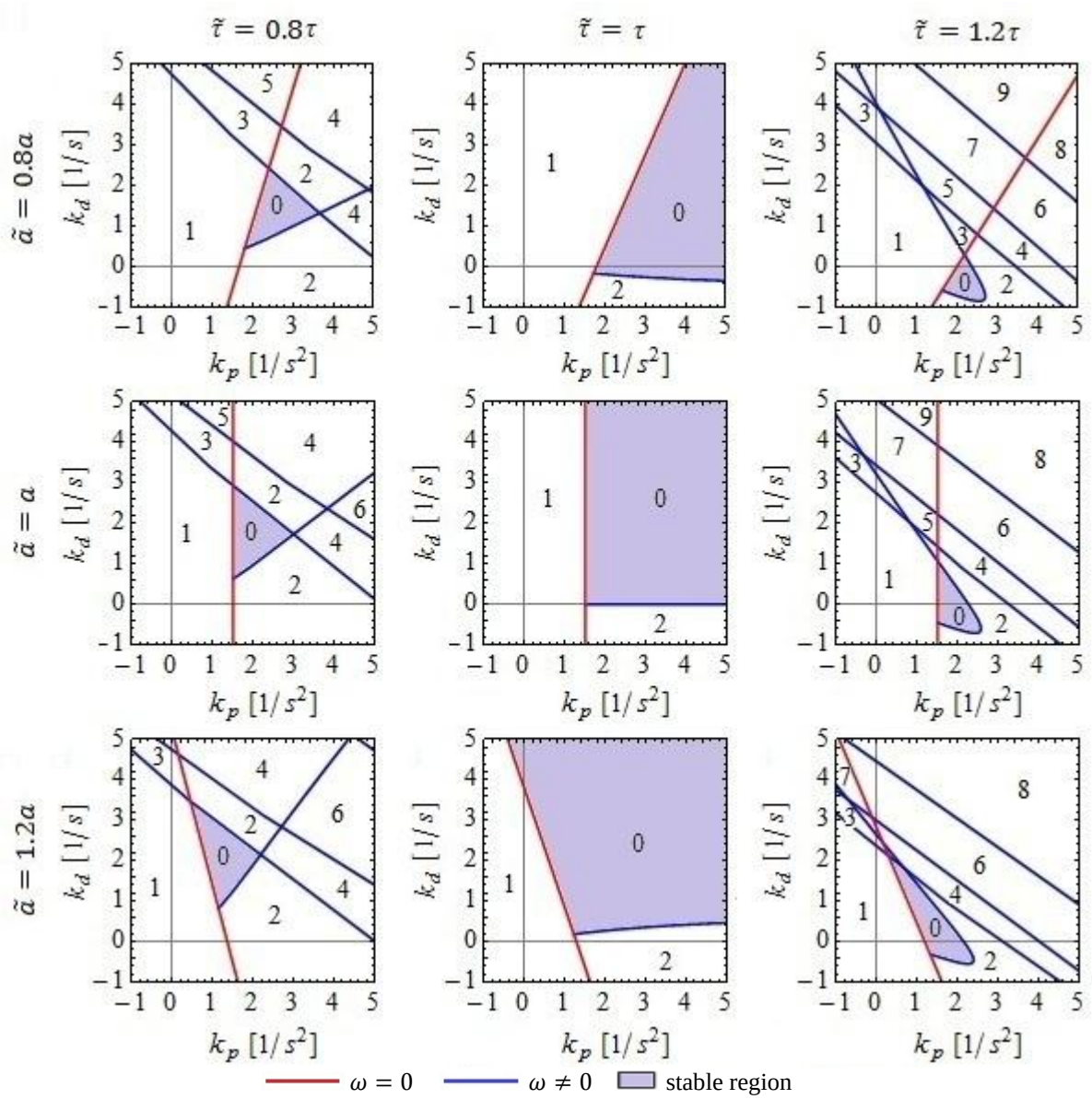

Figure 7. Stability charts of system (3) and (29) with $a = 1.5$ [1/s^2] and $\tau = 1$ [s] for different accuracy of the internal model parameters $\tilde{a}$ and $\tilde{\tau}$.

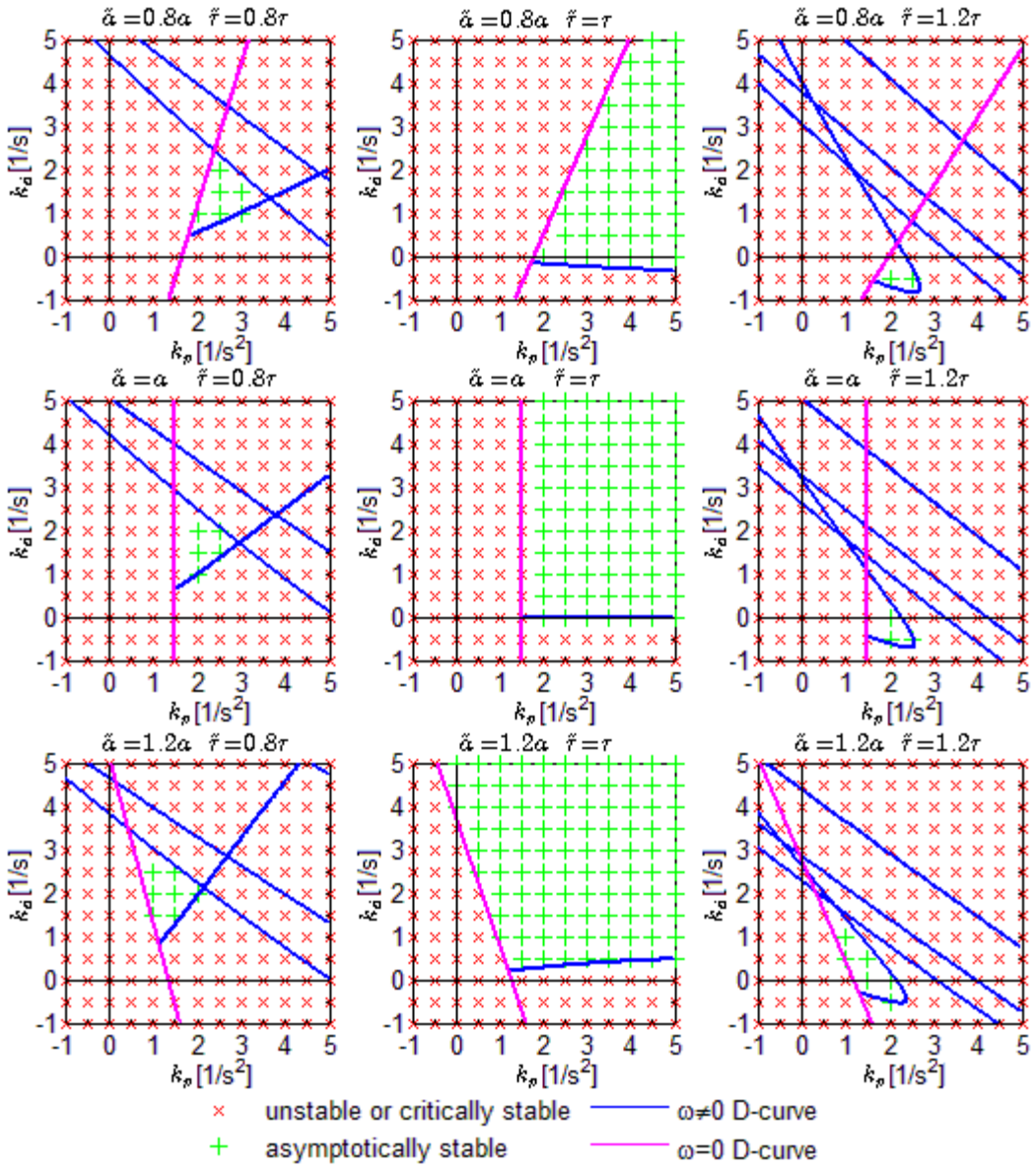

Figure 8. Stability charts of system (45)-(46) with $a = 1.5$ [1/s^2], $\tau = 1$ [s] and $\Delta t = 0.005$ [s] for different accuracy of the internal model parameters $\tilde{a}$ and $\tilde{\tau}$.

6. ANALYSIS OF THE UNCERTAINTIES IN THE PARAMETERS

It has been shown that the precision of the approximation of the system parameters used for prediction affects the stability of the system. If $\tilde{a} = a$ and $\tilde{\tau} = \tau$, then the stable region is a quarter plane in the plane (k_p, k_d). But in the case when $\tilde{a} \neq a$ and $\tilde{\tau} \neq \tau$ the stable region shrinks and becomes bounded. This shows that the control procedure is sensitive to the accuracy of the parameters used for the prediction. This sensitivity can be demonstrated on a series of stability charts shown in Figure 7, where different approximation accuracy is used for the system parameter a and for the feedback delay τ. In this figure the instability degree of each region divided by the D-curves is also presented. The effect of the difference part is not depicted here.

The analysis of the sensitivity with respect to the parameters used for prediction can also be performed in case of the digital controller using the discrete maps (47) and (48). The stability of the system can be determined for discrete points in the plane (k_p, k_d) using the criteria (49). A series of stability charts for the digital control system is shown in Figure 8. The D-curves of the ideal continuous control system is also presented. It is shown that stability of the digital FSA control system approximates well the stability of the ideal continuous control system according to the semi-discretization method [6].

Figure 7 and Figure 8 show that the stability of the control process depends on the accuracy of the parameters $\tilde{a}$ and $\tilde{\tau}$ used by the internal model, which can be characterized by the absolute errors $\varepsilon_a = |a - \tilde{a}|/a$ and $\varepsilon_\tau = |\tau - \tilde{\tau}|/\tau$. For a given

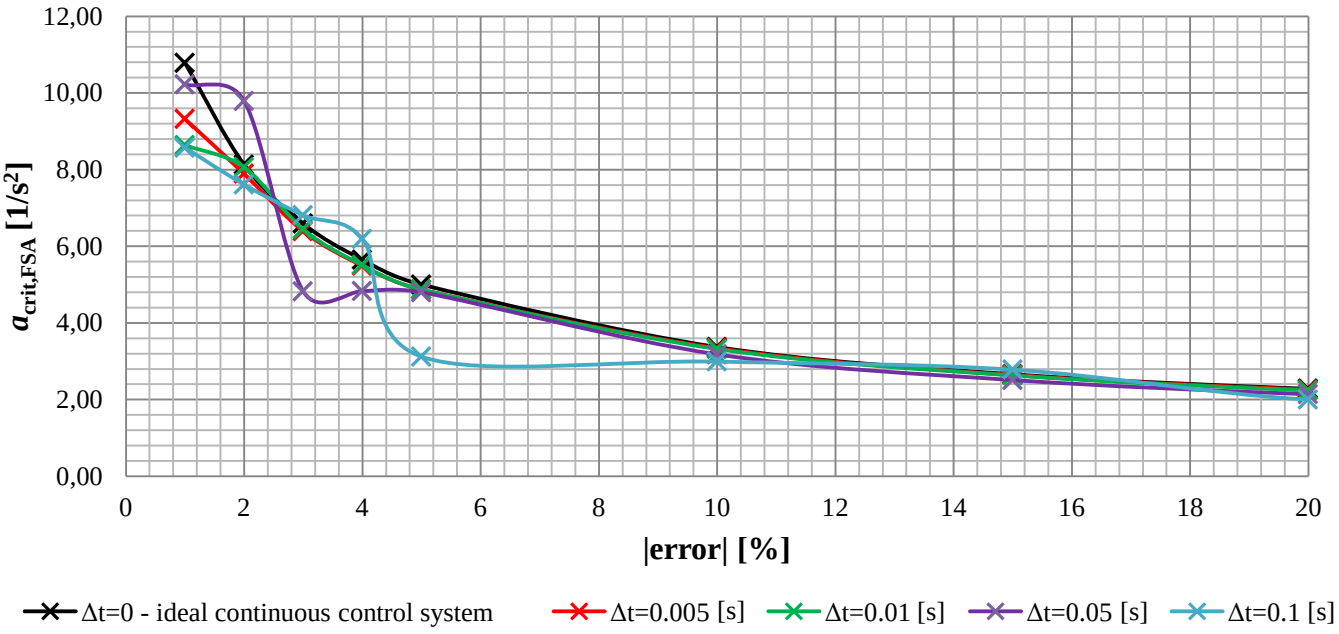

Figure 9. The critical system parameter values as function of the internal model error $\varepsilon = \varepsilon_a = \varepsilon_\tau$ for $\tau = 1$ [s].

feedback delay, the critical value of the system parameter a, for which stabilization is just still possible in the presence of given internal model errors ε_a and ε_τ is denoted by $a_{\text{crit,FSA}}$. Figure 9 presents the critical system parameter $a_{\text{crit,FSA}}$ for different errors $\varepsilon = \varepsilon_a = \varepsilon_\tau$ for actual feedback delay $\tau = 1$ for the ideal continuous control system and for digital controller with different sampling periods Δt. The diagram was determined as follows. The absolute errors ε_a and ε_τ and the system parameter a were fixed and the 3×3 stability charts (shown in Figure 7 and Figure 8) were constructed. The system parameter a was said to be robustly stable against the internal model error $\varepsilon = \varepsilon_a = \varepsilon_\tau$ if there was at least one stable point in the plane (k_p, k_d) in each of the 3×3 stability charts such that the control parameters k_p and k_d were given with accuracy 0.01. If a system parameter a was found to be robustly stable, then it was increased and the same procedure was repeated. A specific value of $a = a_{\text{crit,FSA}}$ was said to be critical if it was robustly stable in the sense described above but the same system for $a = a_{\text{crit,FSA}} + 0.01$ was not robustly stable any more. Thus, the resolution for the system parameter a and the control parameters k_p and k_d were uniformly 0.01 during the analysis.

As it can be seen in Figure 9 the critical system parameter decreases with increasing internal model error. If the internal model is perfectly accurate (i.e. if $\varepsilon = \varepsilon_a = \varepsilon_\tau = 0$) then the theoretical value of $a_{\text{crit,FSA}}$ is infinity, hence the effect of input delay is totally compensated. Note that if $\tau = 1$ then the same critical parameter for a PD controller without any parameter uncertainties is $a_{\text{crit,PD}} = 2$ and for a proportional-derivative-acceleration (PDA) controller it is $a_{\text{crit,PDA}} = 4$ (see [17], [5]). For the FSA controller with good parameter approximation the achievable critical value of $a_{\text{crit,FSA}}$ can be essentially larger than 2 or 4.

Figure 9 also shows that the curve associated with the digital controller tends to the curve of the ideal continuous control system if the sampling period gets smaller and smaller. The oscillations of the curves for $\Delta t = 0.1$ and $\Delta t = 0.05$ are due to the discrete-point analysis over the finite domain of the plane (k_p, k_d) with resolution 0.01.

7. CONCLUSIONS

The inverted pendulum was investigated with input delay subjected to a FSA controller. If the parameters of the internal model used for the prediction are not equal to the real system parameters, then the system is described by Eqs. (3) and (13), which is a system of NFDEs involving two types of delays: a point delay τ and a distributed delay term over a delay period of length $\tilde{\tau}$. For the ideal continuous control system, the stability analysis was performed using the D-subdivision method and the number of unstable characteristic roots were determined using Stepan's formula. The stability of the digital control system was analyzed by constructing the corresponding discrete maps. The stabilizability of the system was investigated for different mismatches between the internal model and the actual system through a series of stability charts. The critical system parameter for which stabilization is just still possible in the presence of internal model errors was determined. It was shown that for internal model errors less than 5%, the critical system parameter $a_{\text{crit,FSA}}$ is almost 5 or more, which is already larger

than the critical system parameter of a PD or a PDA controller without any parameter uncertainty.

The above results were derived for the system parameter $a = 6g/l$ for a unit feedback delay $\tau = 1$. From practical point of view, the results can be demonstrated using the critical length of the inverted pendulum that can be balanced in a stable way. For an actual feedback delay $\tau = 0.1$ s, the minimum length of a pendulum that can be stabilized by an ideal PD controller is $l_{\mathrm{crit,PD}} \cong 29.4$ cm and for an ideal PDA controller it is $l_{\mathrm{crit,PDA}} \cong 14.7$ cm. The critical length for the same system subjected to a FSA controller with 5% internal model error is $l_{\mathrm{crit,FSA,5\%}} \cong 11.8$ cm and for 2% internal model error it is $l_{\mathrm{crit,FSA,2\%}} \cong 7.4$ cm. Thus, the FSA controller extends the limits of stabilization against feedback delay provided that the input signal is available for the control calculation.

ACKNOWLEDGMENTS

This work was supported by the Hungarian National Science Foundation under grant OTKA–K105433.

The work reported in the paper has been developed in the framework of the project „Talent care and cultivation in the scientific workshops of BME" project. This project is supported by the grant TÁMOP-4.2.2.B-10/1--2010-0009.

REFERENCES

[1] Arstein Z, 1982, Linear systems with delayed controls: A reduction, *IEEE Transactions on Automatic Control*, **27**:869-879.

[2] Engelborghs K, Dambrine M, Roose D, 2001, Limitations of a class of stabilization methods for delay systems, *IEEE Transactions on Automatic Control*, **46**(2):336–339.

[3] Gawthrop PJ, Ronco E, 2002, Predictive pole-placement control with linear models, *Automatica*, **38**(3):421–432.

[4] Hajdu D, Insperger T, 2013, Time domain analysis of the Smith Predictor in case of parameter uncertainties: A case study, *Proceedings of the ASME 2013 IDETC/CIE, 9th International Conference on Multibody Systems, Nonlinear Dynamics and Control*, August 4-7, 2013, Portland, OR, USA.

[5] Insperger T, Milton J, Stepan G, 2013, Acceleration feedback improves balancing against reflex delay, *Journal of the Royal Society Interface*, **10**(79):1742-5662.

[6] Insperger T, Stepan G, 2011, *Semi-discretization for time-delay systems*, Springer, New York.

[7] Jankovic M, 2009, Forwarding, backstepping, and finite spectrum assignment for time delay systems, *Automatica*, **45**(1):2-9.

[8] Krstic M, 2009, *Delay compensation for nonlinear, adaptive, and PDE systems*, Birkhäuser, Boston.

[9] Loram ID, Gollee H, Lakie M, Gawthrop PJ, 2011, Human control of an inverted pendulum: Is continuous control necessary? is intermittent control effective? is intermittent control physiological?, *The Journal of Physiology*, **589**(2):307–324.

[10] Manitius AZ, Olbrot AW, 1979, Finite spectrum assignment problem for systems with delays, *IEEE Transactions on Automatic Control*, **AC-24**:541–553.

[11] Michiels W, Mondié S, Roose D, 2003, Robust stabilization of time-delay systems with distributed delay control laws: Necessary and sufficient conditions for a safe implementation, *TWReport 363*, Department of Computer Science, Katholieke Universiteit Leuven, Belgium.

[12] Michiels W, Niculescu S-I, 2007, *Stability and stabilization of time delay systems - An eigenvalue based approach*, SIAM Publications, Philadelphia.

[13] Milton J, Cabrera JL, Ohira T, Tajima S, Tonosaki Y, Eurich CW, Campbell SA, 2009, The time-delayed inverted pendulum: Implications for human balance control, *Chaos*, **19**:026110.

[14] Mondié S, Dambrine M, Santos O, 2002, Approximation of control laws with distributed delays: a necessary condition for stability, *Kybernetika*, **38**(5):541–551.

[15] Moss F, Milton J, 2003, Balancing the unbalanced, *Nature* (London) **425**:911-912.

[16] Palmor ZJ, 2000, Time-delay compensation: Smith predictor and its modifications, in *The Control Handbook*, W.S. Levine, editor, pp. 224 237, Boca Raton, Fl, 2000. CRC and IEEE Press.

[17] Sieber J, Krauskopf B, 2005, Extending the permissible control loop latency for the controlled inverted pendulum, *Dynamical Systems*, **20**(2):189–199.

[18] Smith OJM, 1957, Closer control of loops with dead time, *Chemical Engineering Progress.*, **53**(5):217 219.

[19] Stepan G, 1989, *Retarded dynamical systems*, Longman, Harlow.

[20] Stepan G, 2009, Delay effects in the human sensory system during balancing, *Philosophical Transactions of the Royal Society A*, **367**:1195–1212.

[21] Wang QG, Lee TH, Tan KK, 1999, *Finite spectrum assignment for time delay systems*, Springer.

